Dalton Transactions

H2 Addition to (Me4PCP)Ir(CO): Studies of the Isomerization Mechanism

Journal:	*Dalton Transactions*
Manuscript ID	DT-ART-07-2018-002861.R1
Article Type:	Paper
Date Submitted by the Author:	03-Oct-2018
Complete List of Authors:	Lekich, Travis; Box 351700, Department of Chemistry Gary, J; Stephen F Austin State University College of Liberal and Applied Arts, Department of Chemistry and Biochemistry Bellows, Sarina; University of North Texas, Chemistry Cundari, Thomas; University of North Texas, Chemistry Guard, Louise; Box 351700, Department of Chemistry Heinekey, D; Box 351700, Department of Chemistry

Journal Name

ARTICLE

H_2 Addition to (^{Me4}PCP)Ir(CO): Studies of the Isomerization Mechanism

Received 00th January 20xx,
Accepted 00th January 20xx

DOI: 10.1039/x0xx00000x

www.rsc.org/

Travis T. Lekich[†], J. Brannon Gary[#], Sarina M. Bellows[‡], Thomas R. Cundari[‡,*], Louise M. Guard[†], D. Michael Heinekey[‡,*].

Dedicated to Professor Richard Andersen on the occasion of his 75th birthday.

Reduced steric demand of the ^{Me4}PCP pincer ligand [PCP = κ^3-C_6H_3-2,6-$(CH_2PR_2)_2$ R = Me], allows for a more open metal center. This is evident through structure and reactvity comparisons between (^{Me4}PCP)Ir derivatives and other (^{R4}PCP)Ir complexes (R = ^{t}Bu, ^{i}Pr, CF_3). In particular, isomerization from cis-(^{R4}PCP)Ir(H)$_2$(CO) to trans-(^{R4}PCP)Ir(H)$_2$(CO) is more facile when R = Me than when R = ^{i}Pr. Deuterium incorporation in the hydride ligands from solvent C_6D_6 was observed during this isomerization when R = Me. This deuterium exchange has not been observed for other analogous ^{R4}PCP iridium complexes. A kinetic study of the cis/trans isomerization combined with computational studies suggest that the cis/trans isomerization proceeds through a migratory-insertion pathway involving a formyl intermediate.

Introduction

Several investigations of hydrogenation and dehydrogenation chemistry have employed ^{R4}PCP (κ^3-C_6H_4-1,3-$[CH_2PR_2]_2$) iridium compounds, where R is ^{t}Bu or ^{i}Pr.[3,4] However, there are a limited number of reports of pincer complexes with steric or electronic variation of the phosphine R-groups.[1,5-8] This shortcoming may result from the difficulty in synthesizing ^{R4}PCP ligands where R is neither ^{t}Bu nor ^{i}Pr. We have recently reported a convenient synthesis of ^{Me4}PCP, which has allowed us to explore the coordination chemistry of (^{Me4}PCP)Ir(CO), with particular focus on the oxidative addition of H_2.[10]

Hydrogen addition to square planar iridium complexes is well-studied: H_2 coordinates as a sigma complex, then undergoes oxidative addition to afford a cis-dihydride species.[12] Milstein and coworkers found that (^{iPr4}PCP)Ir(CO) reacts with H_2 to initially form cis-(^{iPr4}PCP)Ir(H)$_2$(CO), but then thermally isomerizes to trans-(^{iPr4}PCP)Ir(H)$_2$(CO).[9] This isomerization was surprising because one would expect that the hydrides would have an energetically unfavorable trans-influence on one another. Through calculations, Hall and co-workers proposed that this thermodynamic preference could be due to a favorable π interaction between the aryl backbone and CO ligand.[13]

We have previously reported that H_2 addition and isomerization also occurs with (^{iPr4}POCOP)Ir(H)$_2$(CO).[4] However, similar complexes with bulkier ligands, (^{tBu4}PCP)Ir(CO) and (^{tBu4}POCOP)Ir(CO), do not oxidatively add H_2 through this mechanism.[4] Roddick and co-workers showed that (^{CF3}PCP)Ir(CO) adds H_2 to initially form cis-(^{CF3}PCP)Ir(H)$_2$(CO) which rapidly isomerizes to trans-(^{CF3}PCP)Ir(H)$_2$(CO).[1] The rate of cis to trans-dihydride isomerization was observed to be much faster at room temperature when R = CF_3 than R = ^{i}Pr.[1,9]

Because the nature of hydrogen addition and elimination is important to understanding aspects of (de)hydrogenation chemistry for which these ^{R4}PCP iridium complexes are commonly used, we compare the reactivity of H_2 with (^{Me4}PCP)Ir(CO) and previously reported (^{R4}PCP)Ir(CO)[1,9,11] complexes to elucidate differences in reactivity that result from the reduced steric profile of ^{Me4}PCP.

Results and Discussion

Synthesis of (^{Me4}PCP)Ir(CO) and Derivatives.

Table 1 shows selected spectroscopic features of compounds **1^{Me}-5^{Me}**, and analogous previously reported compounds. As shown in Scheme 1, ^{Me4}PCP reacts with Ir(CO)$_2$Cl(pyr) at 110 °C to afford (^{Me4}PCP)Ir(HCl)CO, (**1^{Me};** Scheme 1). The ^{1}H NMR spectrum of **1^{Me}** exhibits two doublets of virtual triplets at 3.75 ppm and 3.36 ppm for the inequivalent benzyl protons; two overlapping virtual triplets centered at 1.84 ppm for the methyl protons; and a triplet at -18.8 ppm ($^2J_{HP}$ = 13.9 Hz) for the hydride. The structure of this complex is proposed based upon comparison with previously reported species.[6,9,11] Attempts to metallate ^{Me4}PCP with other precursors, such as [Ir(COE)$_2$Cl]$_2$ and [Ir(COD)$_2$Cl]$_2$, resulted in products insoluble in common organic solvents, even when CO, H_2 or acetonitrile were

[†]Department of Chemistry, University of Washington, Seattle, Washington 98195-1700.
[‡]Department of Chemistry, Center for Advanced Scientific Computing and Modeling (CASCaM), University of North Texas, P.O. Box 305070, Denton, Texas, 76203-5070.
[#]Department of Chemistry & Biochemistry, Stephen F. Austin State University, Nacogdoches, TX 75962.
Electronic Supplementary Information (ESI) available: [details of any supplementary information available should be included here]. See DOI: 10.1039/x0xx00000x

Table 1. Selected Spectroscopic values for compounds 1 - 4.

Compound	^{1}H Ir-*H (ppm)*	$^2J_{HP}$ *(Hz)*	^{31}P {^{1}H} *(ppm)*	ν(*CO*) (*cm^{-1}*)	ν(Ir-*H*) (*cm^{-1}*)	Ref.
1^R: (^{R4}PCP)Ir(HCl)(CO)						
1^{Me}	-18.7[a]	13.8[a]	-2.68[a]	2020[c]	2171[c]	-
1^{iPr}	-18.3[e]	11.6[e]	50.8[e]	2010[d]	2197[d]	9
1^{tBu}	-7.60[g]	15.0[g]	56.1[g]	1994[f]	2165[f]	11
1^{CF3}	-16.5[a]	14.4[a]	56.7[a]	2091[c]	N/A	6
2^R: (^{R4}PCP)Ir(CO)						
2^{Me}	-	-	17.1[a]	1933[a]	-	-
2^{iPr}	-	-	66.2[a]	1920[c]	-	4
2^{tBu}	-	-	82.9	1913[d]	-	4
2^{CF3}	-	-	69.7[a]	2018[c]	-	1
trans-3^R: trans-(^{R4}PCP)Ir(H)$_2$(CO)						
trans-3^{Me}	-9.16[a]	16.4[a]	-6.08[a]	1992[c]	1722[c]	-
trans-3^{iPr}	-9.69[e]	15.0[e]	57.8[e]	1978[d]	1746[d]	9
trans-3^{CF3}	-9.10[a]	19.2[a]	59.7[a]	2068[c]	2090[c]	1
cis-3^R: cis-(^{R4}PCP)Ir(H)$_2$(CO)						
cis-3^{Me}	-9.85[a]	19.4[a]	-15.6[a]	[a]	2055[a]	-
	-11.1[a]	12.6[a]			1950[a]	
cis-3^{iPr}	-10.9[a]	16.9[a]	51.7[e]	1950[d]	2066[d]	9
	-11.9[a]	11.9[a]			1965[d]	
4^R: [(^{R4}PCP)Ir(H)(pyr)(CO)]$^+$						
4^{Me}	-19.4[c]	16.4[c]	1.07[c]	2032[c]	2182[c]	-
4^{iPr}	-19.1[a]	12.0[a]	47.8[a]	2023[c]	N/A	4
4^{tBu}	-19.7[a]	14.0[a]	60.8[a]	2018[c]	N/A	4
5^{Me}: (^{R4}PCP)Ir(CO)$_2$						
5^{Me}	-	-	-	2010[a], 1920[a]	-	-
5^{CF3}	-	-	-	2068[c], 2020[c]	-	1

[a]In C_6D_6. [b]In toluene-d_8. [c]In CH_2Cl_2 or CD_2Cl_2. [d]Film. [e]Solvent not specified. [f]Nujol mull. [g]In $CDCl_3$.

present.[4,11] These presumably polymeric materials form because smaller pincer ligands tend to form oligomers with metal precursors and/or the methyl groups may become activated by coordinatively unsaturated iridium species.[14-16]

LiHMDS dehydrohalogenates **1^{Me}** to afford (^{Me4}PCP)Ir(CO), (**2^{Me}**; Scheme 2). The ^{1}H NMR spectrum of **2^{Me}** shows a virtual triplet at 3.07 ppm for the benzyl protons, and a virtual triplet at 1.23 ppm for the methyl protons.

Compound **1^{Me}** undergoes reaction with $NaBH_4$ in a 1:1 mixture of EtOH/MeCN to afford trans-(^{Me4}PCP)Ir(H)$_2$CO, (**trans-3^{Me}**; Scheme 3). The ^{1}H NMR spectrum of the dihydride complex shows a virtual triplet at 3.21 ppm for the benzyl protons, a virtual triplet at 1.49 ppm for the methyl protons, and a triplet at -9.16 ppm($^2J_{HP}$ = 16.4 Hz) for the hydrides.

One equivalent of pyridinium triflate [Hpyr][OTf] protonates **2^{Me}** to afford [(^{Me4}PCP)Ir(H)(pyr)CO][OTf], **4^{Me}** (Scheme 4). The ^{1}H NMR spectrum of **4^{Me}** shows three sharp signals for bound pyridine (8.16 (d), 7.97 (t), 7.39 (t) ppm), two doublets of virtual triplets at 3.57 and 3.44 ppm for the diastereotopic benzyl protons, two virtual triplets at 1.97 and 1.39 ppm for the methyl protons, and a triplet at -19.35 ($^2J_{HP}$ = 16.4 Hz) for the hydride.

Compound **2^{Me}** coordinates CO under 1 atm CO at room temperature to afford (^{Me4}PCP)Ir(CO)$_2$ (**5^{Me}**; Scheme 5a). The ^{1}H and ^{31}P{^{1}H} NMR spectra of **5^{Me}** are shifted relative to **2^{Me}** (Supplementary Material, Figures S17, S18). Compound 2^{Me} also coordinates PMe_3 to give (^{Me4}PCP)Ir(PMe_3)(CO) (**6^{Me}**; Scheme 5b). The ^{31}P{^{1}H} NMR spectrum of **6^{Me}** shows a doublet at -1.79 ppm and triplet at -56.5 ppm ($^2J_{PP}$ = 112 Hz). Heating 6^{Me} to 80 °C in toluene-d_8 does not result in conversion to a new species.

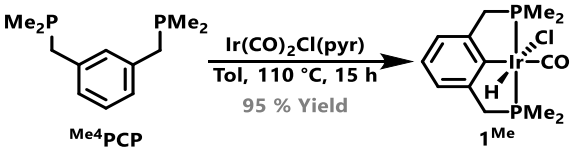

Scheme 1 The synthesis of (^{Me4}PCP)Ir(HCl)CO **1^{Me}**.

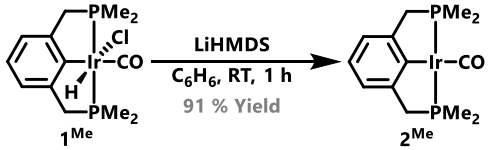

Scheme 2 Synthesis of (^{Me4}PCP)Ir(CO) **2^{Me}**.

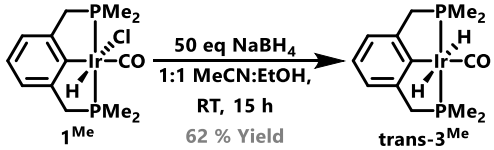

Scheme 3 Synthesis of trans-(^{Me4}PCP)Ir(H)$_2$(CO) **3^{Me}**.

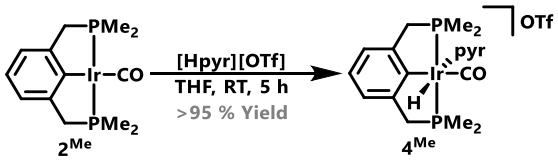

Scheme 4 Synthesis of [(^{Me4}PCP)Ir(H)(pyr)(CO)]$^+$(**4^{Me}**).

Table 2 Space-filling models of the crystal structures for $\mathbf{2^{Me}}$, $\mathbf{2^{iPr}}$, $\mathbf{2^{tBu}}$, and $\mathbf{2^{CF3}}$.

(^{R4}PCP)Ir(CO) R =	Me ($\mathbf{2^{Me}}$)	^{i}Pr ($\mathbf{2^{iPr}}$)	^{t}Bu ($\mathbf{2^{tBu}}$)[16]	CF_3 ($\mathbf{2^{CF3}}$)[4]
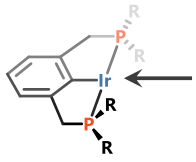	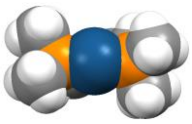	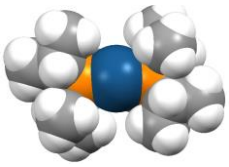	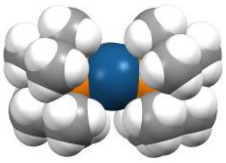	
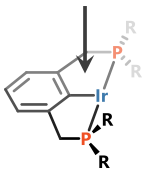		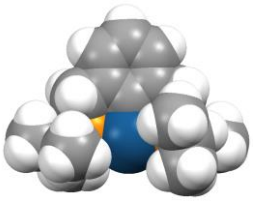	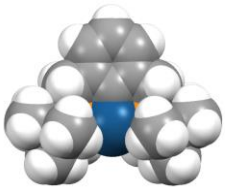	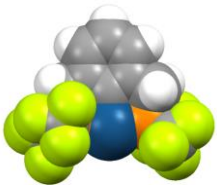

The CO ligands are omitted for clarity. The structures of $\mathbf{2^{tBu}}$ and $\mathbf{2^{CF3}}$ were previously reported.[1,2]

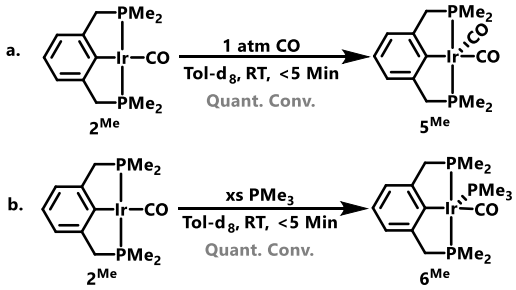

Scheme 5. Synthesis of (^{Me4}PCP)Ir(CO)$_2$ $\mathbf{5^{Me}}$ (a) and (^{Me4}PCP)Ir(PMe_3)(CO) $\mathbf{6^{Me}}$ (b).

Compound $\mathbf{2^{Me}}$ coordinates CO under 1 atm CO at room temperature to afford (^{Me4}PCP)Ir(CO)$_2$ ($\mathbf{5^{Me}}$; Scheme 5a). The ^{1}H and ^{31}P{^{1}H} NMR spectra of $\mathbf{5^{Me}}$ are shifted relative to $\mathbf{2^{Me}}$ (Supplementary Material, Figures S17, S18). Compound $\mathbf{2^{Me}}$ also coordinates PMe_3 to give (^{Me4}PCP)Ir(PMe_3)(CO) ($\mathbf{6^{Me}}$; Scheme 5b). The ^{31}P{^{1}H} NMR spectrum of $\mathbf{6^{Me}}$ shows a doublet at -1.79 ppm and triplet at -56.5 ppm ($^{2}J_{PP}$ = 112 Hz). Heating $\mathbf{6^{Me}}$ to 80 °C in toluene-d_8 gives no change in the NMR spectrum. NMR spectroscopy (^{1}H and ^{31}P{^{1}H}) shows no evidence for interaction of excess pyridine with $\mathbf{2^{Me}}$.

Steric Comparison of Compounds 1 - 4.

Table 2 shows the space-filling models and Table 3 shows select structural values of compounds $\mathbf{2^{Me}}$, $\mathbf{2^{iPr}}$, $\mathbf{2^{tBu}}$, $\mathbf{2^{CF3}}$.[1,2] As expected, $\mathbf{2^{Me}}$ has the lowest buried volume (%V_{bur})[17] among the set of complexes. Like $\mathbf{2^{CF3}}$, $\mathbf{2^{Me}}$ has a large C_2 twist as measured by the dihedral angle between the CH_2-C_{Ar}-CH_2 and P-Ir-P planes.[7] This C_2 twist is more pronounced for sterically small PCP ligands coordinated to square planar iridium complexes because of the reduced steric clash between phosphine groups.[7] Compound $\mathbf{2^{Me}}$ also has a relatively small P-M-P angle, which is congruent with a lower %V_{bur} and larger C_2 twist.[7] The pyridine dynamics on the NMR time scale in compounds $\mathbf{4^{Me}}$, $\mathbf{4^{iPr}}$, $\mathbf{4^{tBu}}$ can be used as proxy for understanding the steric environment in the void space perpendicular to the P-Ir-P plane. The ^{1}H NMR spectrum of $\mathbf{4^{Me}}$ shows three sharp resonances for bound pyridine (Supplementary Material, Figure S14). In contrast, the ^{1}H NMR spectrum of $\mathbf{4^{tBu}}$ shows five sharp signals for bound pyridine, and the ^{1}H NMR spectrum of $\mathbf{4^{iPr}}$ shows three broad signals for bound pyridine.[2] The spectral differences suggest that the pyridine ligand of compound $\mathbf{4^{Me}}$ freely rotates, the pyridine ligand of $\mathbf{4^{iPr}}$ undergoes hindered rotation, and the pyridine ligand of $\mathbf{4^{tBu}}$ is static on the NMR time-scale. The differences in the pyridine's rotation is most likely due to its steric interactions with the respective PCP ligands.

Electronic Comparison of Compounds 1-5.

Here, we use the CO stretching frequency v(CO) as an approximate representation of the electronic character at the iridium center. The Ir-CO and Ir-H stretching frequencies are presented in Table 1. The v(CO) of the ^{Me4}PCP iridium complexes are slightly higher in energy than the ^{iPr4}PCP and ^{tBu4}PCP analogues because methyl groups are less electron donating than tert-butyl and iso-propyl groups. However, the electronic differences among the aliphatic-substituted complexes are not very pronounced, so one should not expect large electronic differences among the methyl, tert-butyl and iso-propyl substituted complexes. By contrast, the CF_3-substituted complexes are electron deficient compared to the aliphatic series, and one should expect significant electronic differences between the methyl and CF_3-substituted complexes that are reflected in much higher v(CO) values. (Table 1)

Table 3 Select Structural Data for (^{R4}PCP)Ir(CO) (2^{R}).

2^R	$\%V_{bur}$[a]	Twist[b] (°)	P-M-P (°)
2^{Me}	55.7	16.2(5), 17.2(5)	160.61(9)
2^{iPr}	67.6	8.0(3), 10.4(3)	163.71(4)
2^{tBu}	72.2	5.1(7), 1.0(7)	164.11(12)
2^{CF3}	61.4	12.5(14)	159.86 (2)

[a]Calculated for the PCP ligand fragment with SambVca 2.0.[17] [b]The dihedral angle between the aryl plane and Ir-P bond.

Hydrogen Addition to 2^{Me}

Compound $\mathbf{2^{Me}}$ oxidatively adds H_2 under one atmosphere of H_2 at room temperature in toluene-d_8 to initially form cis-(^{Me4}PCP)Ir(H)$_2$(CO) (**cis-3^{Me}**), then isomerizes to **trans-3^{Me}** (Scheme 6). The isomerization reaches equilibrium after about 1 day at room temperature and under 1 atm H_2 (ΔG_{298} = -2.5 kcal/mol). Kinetic analysis, conducted under 1 atm H_2, suggests that this isomerization is first-order in **cis-3^{Me}** (see Supplementary Material).

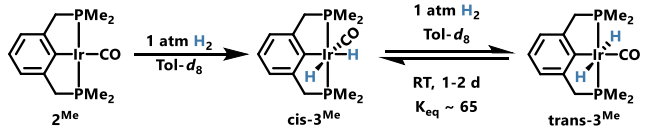

Scheme 6 H_2 Addition to $\mathbf{2^{Me}}$ gives **cis-3^{Me}**, which isomerizes to **trans-3^{Me}**.

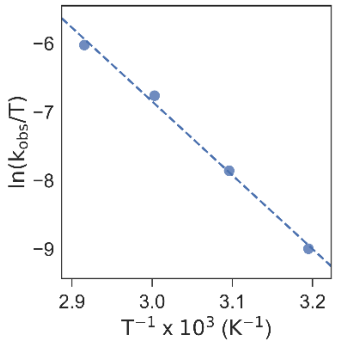

$\Delta H^{\ddagger}$	21.2 ± 1.3 kcal/mol
$\Delta S^{\ddagger}$	-8.84 ± 3.9 cal/mol
$\Delta G^{\ddagger}_{273}$	23.6 ± 2.2 kcal/mol

Fig. 1 Eyring plot and thermodynamic values for the isomerization of **cis-3^{Me}** to **trans-3^{Me}** under 1 atm H_2.

Figure 1 shows the Eyring plot and extracted thermodynamic values for the the **cis/trans-3^{Me}** isomerization**.**

Density functional theory (DFT) studies were employed to gain insights into the mechanism. The quantum model combined the PBE0 functional with the 6-311G(d,p) basis set on all main group atoms and the LANL2DZ valence basis set with an effective core potential for Ir. This level of theory has been used with success in previous theory-experiment studies of Ir-pincer chemistry.[18-22] The cis to trans equilibrium was first investigated. Consistent with experiment, the trans isomer is calculated to be more stable by 3.8 kcal/mol (free energy) compared to the experimental observation of 2.5 kcal/mol (*vide supra*). In an effort to provide a plausible mechanism for the cis- to trans- conversion, multiple pathways were evaluated which contain significant barriers, such as a Bailar twist ($\Delta G^{\ddagger}_{calcd}$ = +42 kcal/mol), and Ar-H reductive elimination followed by ring inversion ($\Delta G^{\ddagger}_{calcd}$ = +60 kcal/mol). However, a migratory insertion pathway to form a formyl intermediate showed reasonable agreement to the experimental activation parameters (Figure 2).

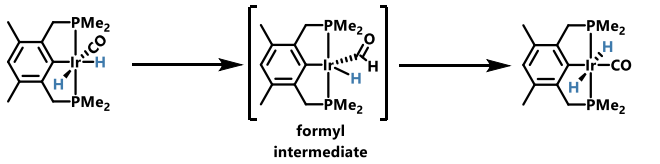

Fig. 2 Computed migratory insertion pathway.

The most plausible mechanism studied involves the migratory insertion of a hydride ligand and the carbonyl ligand, producing a formyl intermediate. The transition state to form the formyl intermediate has $\Delta G^{\ddagger}_{calcd}$ = +26.7 kcal/mol and the formyl intermediate has a free energy of +19.5 kcal/mol above the reactants. From the formyl intermediate, a de-insertion (transition state free energy = +29.9 kcal/mol) leads to the formation of the more stable trans product.

Qualitatively, **2^{iPr}**, **2^{CF3},** and **2^{Me}** oxidatively add H_2 at a similar rate to form **cis-3^{R}** under 1 atm H_2.[1,9] However, the qualitative rate of isomerization from **cis-3^{R}** to **trans-3^{R}** differs for different R groups.[4,10] Compound **cis-3^{CF3}** is only observable at low temperatures under 1 atm H_2, whereas **cis-3^{iPr}** can only be converted to **trans-3^{iPr}** at 100 °C and under 2.4 atm H_2.[1,9] Sterically, methyl groups are smaller than iso-propyl groups, but similar in size to CF_3 groups. Thus, the qualitative rate of isomerization from **cis-3^{R}** to **3^{R}** must be due to coupled steric and electronic factors imposed upon these systems by the PCP ligand.

Unlike previous studies of H_2 addition involving **2^{tBu}**, **2^{iPr}**, and **2^{CF3}** all of which use C_6D_6 as the solvent, we found that heating **cis-3^{Me}** under 1 atm H_2 in C_6D_6 at 80 °C to equilibrium affords a mixture of **trans-3^{Me}** and **trans-3^{Me-d}** (25 % of **3^{Me}**). Similar reactivity is also observed when heating **trans-3^{Me}** under 1 atm H_2 in C_6D_6 at 80 °C. Compound **trans-3^{Me-d}** was characterized by a new ^{1}H NMR hydride signal at -9.06 ppm (t; $^2J_{HP}$ = 16.4 Hz) in C_6D_6. An increase in the intensity of the residual protio-solvent signal due to C_6D_5H was also observed. All other NMR signals are identical between **trans-3^{Me-d}** and **trans-3^{Me}**. Furthermore, the presence of **trans-3^{Me-d}** was confirmed with comparison with an independently synthesized mixture of **trans-3^{Me-d}** and **trans-3^{Me}**. A mixture of **trans-3^{Me-d}** and **trans-3^{Me}** can be synthesized by treating **1^{Me}** with $NaBD_4$ in an analogous preparation to the synthesis of **trans-3^{Me}**.. No significant H/D exchange was observed after equilibrium was reached. This suggests that the degree of H/D exchange is correlated with the concentration of **cis-3^{Me}** and by extension with the concentration of an intermediate species**.** A species with an open coordination site which may form during the isomerization is likely responsible for this observed H/D exchange. We did not observe any H/D exchange between **cis-3^{Me}** and **trans-3^{Me}** in toluene-d_8 up to 80 °C, or in the presence of pyridine or $NaBF_4$ in C_6D_6.

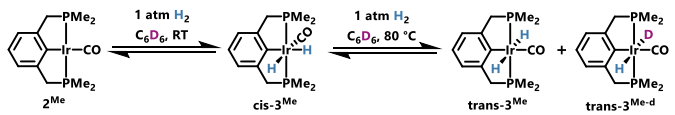

Scheme 7. H/D exchange with C_6D_6 during the isomerization of **cis-3^{Me}** to **trans-3^{Me}**.

Compound **cis-3^{Me}** slowly converts to both **2^{Me}** and **trans-3^{Me}** upon removal of the H_2 atmosphere at room temperature. This suggests that the rates of H_2 loss from **cis-3^{Me}** and the isomerization of **cis-3^{Me}** to **trans-3^{Me}** are comparable, and that **cis-3^{Me}** is in equilibrium with **2^{Me}** and H_2. Compound **trans-3^{Me}** is stable when not under an H_2 atmosphere, though it loses H_2 when heated to 80 °C under static vacuum in solution.

To further elucidate a possible mechanism for this isomerization, we introduced additives to the isomerization under 1 atm H_2. Figure 3 compares the isomerization rates at 40 °C with an added L-type ligand (pyridine) and Lewis acid ($NaBF_4$). Both the pyridine and $NaBF_4$ accelerate the isomerization. Because an L-type ligand increases the rate of reaction, we hypothesize that CO dissociation is unlikely during isomerization. As well, a previously proposed Bailar Twist mechanism would be unaffected by added ligands or Lewis acids.[10,11] A reductive elimination (followed by an inversion) may be facilitated by an L-type ligand, however, a Lewis acid should not affect this mechanism. The only mechanistic pathway that would plausibly be accelerated by a L-type ligand and a Lewis acid is a migratory insertion pathway. Consistent with our interpretation, calculations indicate that the binding of pyridine to the 5-coordinate formyl intermediate (*vide supra*) stabilizes the intermediate to a free energy of +10.6 kcal/mol (in comparison to +19.5 kcal/mol for the 5-coordinate intermediate). This significant stabilization provides a rationale for the increased isomerization rate observed experimentally.

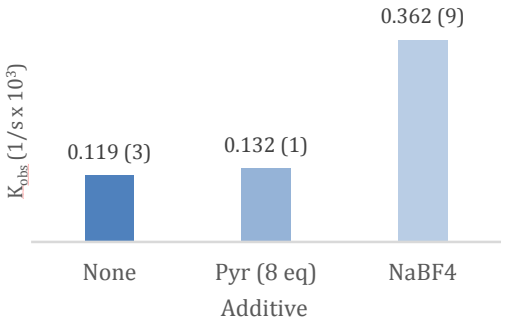

Fig. 3 The effect of additives on the isomerization rate of **2^{Me}** to **trans-3^{Me}** at 40 °C under 1 atm H_2.

We hypothesized that a strongly coordinating ligand may trap an intermediate iridium species with an open coordination site if one is formed during the isomerization from **cis-3^{Me}** to **trans-3^{Me}**. Table S9 (Supplementary Material) summarizes the reactivity of **cis-3^{Me}** and **trans-3^{Me}** with strong ligands (PMe_3, or tert-butyl isonitrile) under 1 atm H_2. The attempts with tert-butyl isonitrile led to intractable products which likely came about through exchange between the original CO ligand and the isonitrile. Reactions involving **6^{Me}** or **trans-3^{Me}** and PMe_3 under 1 atm H_2 led to exchange between CO and PMe_3 to afford one predominant species with ^{1}H and ^{31}P{^{1}H} NMR spectroscopic features consistent with assignment to trans-(^{Me4}PCP)Ir(H)$_2$(PMe_3) (**trans-7^{Me}**). A crystal structure of **trans-7^{Me}** is shown in Figure S24 (Supplementary Material). Adding PMe_3 directly to **cis-3^{Me}** under 1 atm H_2 resulted in H_2 elimination and PMe_3 coordination to afford **6^{Me}**. Reactions involving added CO either resulted in loss of H_2 (with excess CO) or rapid isomerization (ca. 1 eq of CO). These reactions were unsuccessful at trapping an intermediate species.

CONCLUSIONS

Reducing the steric bulk of the PCP ligand has a significant effect on the reactivity of (^{R4}PCP)Ir(CO) complexes and their derivatives. In the series where R is ^{t}Bu, ^{i}Pr, or Me, decreasing the size of the R group allows species to interact with the metal center under more facile conditions, allowing for previously unobserved reactivity. The kinetic, experimental, and computational data suggest that the **cis/trans-3^{Me}** isomerization proceeds through a migratory insertion pathway.

EXPERIMENTAL

General Considerations. All manipulations and reactions used standard Schlenk techniques under an argon atmosphere unless otherwise stated. Glassware and diatomaceous earth were stored in an oven maintained at 140 °C for at least 24 h prior to use. All protio solvents were passed through activated alumina and activated 3Å molecular sieves prior to use. Deuterated solvents were dried over calcium hydride (CD_2Cl_2), sieves (THF-d_8), or sodium (C_6D_6, Tol-d_8), and vacuum transferred prior to use. ^{1}H, ^{31}P{^{1}H}, and ^{13}C{^{1}H} NMR spectra were recorded on a Bruker AV-300, AV-500, DRX-500, or AV-700 instrument. 1H NMR and ^{13}C{^{1}H} NMR spectra were referenced to residual solvent signals.[23] ^{31}P{^{1}H} NMR spectra were referenced to an 85% H_3PO_4 standard. Elemental analysis was completed at the CENTC facility at the University of Rochester (funded by NSF CHE-0650456. Ir(CO)$_2$Cl(pyr)[24] and ^{Me4}PCP[10] were synthesized as previously reported. Formatted tables of the characterization data can be found in the supplementary information.

1^{Me}: (^{Me4}PCP)Ir(HCl)CO. Ir(CO)$_2$Cl(pyr) (0.505g, 1.54 mmol) was added to a solution of ^{Me4}PCP (0.350 g, 1.54 mmol) in toluene (15 mL). The addition was accompanied by effervescence, and an abundant precipitate. The mixture was heated at 110 °C for 15 h, resulting in a yellow solution. The solution was filtered through diatomaceous earth to remove trace particulates. The volatiles were removed under vacuum to afford a white powder. The white powder was triturated with pentane (3 x 1 mL), and then dried under vacuum to afford (^{Me4}PCP)Ir(HCl)CO (0.704 g, 1.46 mmol, 95 % yield).. ^{1}H NMR (300 MHz, CD_2Cl_2): δ 7.07 (d; $^3J_{HH}$ = 7.5 Hz; 2H; Ar-*H*), 6.93 (t; $^3J_{HH}$ = 7.5 Hz; 1H; Ar-*H*), 3.80-3.30 (m; 4H, Ar(-C*H*$_2$-)), 1.84 (m; 12H, -P(C*H*$_3$)), -18.8 (t; $^2J_{HP}$ = 13.8 Hz; 1H; Ir-*H*). ^{31}P{^{1}H} NMR (121 MHz, CD_2Cl_2): δ -2.68. ^{13}C{^{1}H} NMR (126 MHz, C_6D_6): δ 178.4 (s; Ir-CO), 147.3 (s; C_{Ar}),

125.1 (s; C_{Ar}), 122.7 (s; C_{Ar}), 46.0 (vt; -(CH_2)-), 17.7 (vt; P(CH_3)), 11.8 (vt; P(CH_3)). IR (solution, CH_2Cl_2, cm^{-1}) ν(CO) 2020, ν(Ir-H) 2171. Calc: C 32.40; H 4.18, Found: C 33.57; H 4.12.

2^{Me}: (^{Me4}PCP)Ir(CO). (^{Me4}PCP)Ir(HCl)(CO) (**1^{Me}**) (0.22 g, 0.46 mmol) and KHMDS (0.092 g, 0.46 mmol) were stirred in benzene for 1 hour at room temperature. The mixture was filtered through diatomaceous earth, and then the solvent was removed under vacuum to afford (^{Me4}PCP)Ir(CO) (0.188 g, 0.42 mmol, 91 % yield). X-ray diffraction quality crystals of (^{Me4}PCP)Ir(CO) were grown from slow evaporation of a concentrated solution of (^{Me4}PCP)Ir(CO) in pentane at -35 °C over a 7 days. ^{1}H NMR (300 MHz, C_6D_6): δ 7.17 (d; $^3J_{HH}$ = 7.3 Hz; 2H; Ar-*H*), 7.09 (t; $^3J_{HH}$ = 7.3 Hz; 1H; Ar-*H*), 3.07 (vt; 4H; Ar(-CH_2-)), 1.84 (vt; 12H; -P(CH_3)). ^{31}P{^{1}H} NMR (121 MHz, C_6D_6): δ 17.1. ^{13}C{^{1}H} NMR (126 MHz, C_6D_6): δ 196.8 (m; Ir-CO), 180.8 (m; C_{Ar}), 152.9 (m; C_{Ar}), 126.3 (m; C_{Ar}), 121.3 (m; C_{Ar}), 47.7 (vt, -(CH_2)-), 16.9 (vt, -P(CH_3)). IR (solution, C_6D_6, cm^{-1}). Calc: C 35.05; H 4.03; Found C 34.67; H 4.04.

trans-3^{Me}: trans-(^{Me4}PCP)Ir(H)$_2$(CO). $NaBH_4$ (0.416 g, 11.0 mmol) and (^{Me4}PCP)Ir(HCl)CO (0.106 g, 0.220 mmol) were stirred in 1:1 ethanol (10 mL): acetonitrile (10 mL) in a 50 mL Schlenk tube. The solvent was removed under vacuum, resulting in a white solid. The solid was extracted with benzene and the mixture was filtered through diatomaceous earth. The solvent was removed under vacuum to give a white solid, which was washed with cold (-35 °C) pentane to afford (^{Me4}PCP)Ir(H)$_2$CO (0.061g, 0.136 mmol, 62 % yield). ^{1}H NMR (300 MHz, C_6D_6): δ 7.09 (m; 3H; Ar-*H*), 3.14 (vt; 4H; Ar(-CH_2-)), 1.42 (vt; 12H, -P(CH_3)), -9.23 (t; $^2J_{HP}$ = 16.4; 2H; Ir-*H*). ^{31}P{^{1}H} NMR (121 MHz, C_6D_6): δ -6.08. ^{13}C{^{1}H} NMR (126 MHz, C_6D_6): δ 179.8 (s; Ir-*C*O), 153.6 (s; C_{Ar}), 146.2 (s; C_{Ar}), 123.1 (s; C_{Ar}), 122.0 (s; C_{Ar}), 50.3 (vt; -(CH_2)-), 20.9 (vt; P(CH_3)). IR (solution, C_6D_6, cm^{-1}) ν(*CO*) 1992, ν(*Ir-H*) 1722. Calc: C 34.89; H 4.73 Found C 35.78; H 4.77.

cis-3^{Me}: cis-(^{Me4}PCP)Ir(H)$_2$(CO). A J-Young NMR tube was charged with (^{Me4}PCP)Ir(CO) (**2^{Me}**) (ca. 5 mg, 0.01 mmol) and C_6D_6. The solution was degassed, then introduced to 1 atm H_2. The J-Young NMR tube was vigorously shaken for 20 seconds. ^{1}H and ^{31}P{^{1}H} NMR spectra were recorded ca. 5 minutes after H_2 addition. ^{1}H NMR (300 MHz, C_6D_6): 7.16 (m; 3H; *Ar*), 3.18 (vt; 4H; -CH_2-), 1.40 (vt; 6H; P(CH_3)$_2$), 1.36 (vt; 6H; P(CH_3)$_2$), -9.85 (t; $^2J_{HP}$ = 19.2 Hz; 1H), -11.0 (t; $^2J_{HP}$ = 12.4 Hz; $^2J_{HH}$ = 3.0 Hz 1H). ^{31}P{^{1}H} NMR (121 MHz, C_6D_6): δ -12.3. IR (solution, C_6D_6, cm^{-1}) ν(*CO*) 2010, ν(*Ir-H*) 2055, 1950.

4^{Me}: [(^{Me4}PCP)Ir(H)(pyr)CO][OTf]. (^{Me4}PCP)Ir(CO) (42 mg, 0.09 mmol) and pyridinium triflate (15 mg, 0.09 mmol) were stirred in THF (1 mL) in a scintillation vial for 5 h. The precipitate was removed by filtration through diatomaceous earth, then the volatiles were removed under vacuum. The resulting off-white solid was washed with benzene, then the volatiles were removed under vacuum to afford [(^{Me4}PCP)Ir(H)(pyr)CO][OTf] (54 mg, 0.08 mmol, 95 % yield). ^{1}H NMR (300 MHz, CD_2Cl_2): δ 8.09 (d; $^3J_{HH}$ = 5.2 Hz; 2H; C_5H_5N), 7.89 (t; $^3J_{HH}$ = 7.45 Hz; 1H; C_5H_5N), 7.32 (app t; 2H; C_5H_5N), 7.17 (m; 2H; Ar-*H*), 7.09 (m; 1H; Ar-*H)*, 3.55-3.32 (m; 4H; Ar(-CH_2-)), 1.89 (vt; 6H; -P(CH_3)$_2$), 1.31 (vt; 6H; -P(CH_3)$_2$), -19.4 (t; $^3J_{HH}$ = 14.2 Hz 1H; Ir-*H*). ^{31}P{^{1}H} NMR (121.5 MHz, CD_2Cl_2): δ 1.07. ^{13}C{^{1}H} NMR (176 MHz, CD_2Cl_2): δ 177.3 (s; Ir-*C*O), 157.9 (s; C_{Ar}), 154.1 (s; C_{Ar}), 147.9 (t; $^3J_{CP}$ = 7.5 Hz; C_{Ar}), 140.1 (s; C_{Ar}), 128.0 (s; C_{Ar}), 127.3 (s; C_{Ar}), 124.6 (t; $^3J_{CP}$ = 8.6 Hz; C_{Ar}), 45.5 (vt; -(CH_2)-), 19.0 (vt; P(CH_3)), 16.1 (vt; P(CH_3)). IR (solution, CD_2Cl_2, cm^{-1}) ν(*CO*) 2032, ν(*Ir-H*) 2183. Calc: C 33.83; N 2.08; H 3.74, Found: C 33.82; N 2.11; H 3.57

5^{Me}: (^{Me4}PCP)Ir(CO)$_2$. A solution of (^{Me4}PCP)Ir(CO) (**2^{Me}**) (ca. 5 mg, 0.01 mmol) in toluene-d_8 (0.350 mL) was pressurized with 1 atm of CO. The solution was vigorously shaken and turned from yellow to colorless. The spectral features are consistent with assignment to **5^{Me}**. Upon removal of the solvent under vacuum, **5^{Me}** loses CO to afford **2^{Me}**.Compound **5^{Me}** is metastable when not under a CO atmosphere. ^{1}H NMR (300 MHz, Tol-d_8): δ 7.10 – 6.98 (m; 3H; Ar-*H*); 3.07 (vt; 4H; Ar(-CH_2-), 1.34 (vt; 12H; -P(CH_3)). ^{31}P{^{1}H} NMR (121 MHz, Tol-d_8) δ -5.77 (s). ^{13}C{^{1}H} NMR (176 MHz, Tol-d_8) 186.6 (s; Ir-*C*O), 147.1 (t; $^2J_{CP}$ = 7.9 Hz; C_{Ar}), 122.9 (s; $_{CAr}$), 121.0 (s; C_{Ar}), 51.2 (vt; -(CH_2)-), 18.8 (vt; P(CH_3)). IR (solution, C_6D_6, cm^{-1}) ν(*CO*) 2010, 1930.

6^{Me}: (^{Me4}PCP)Ir(CO)(PMe$_3$). A J-Young NMR tube was charged with (^{Me4}PCP)Ir(CO) (ca. 5 mg, 0.01 mmol) in toluene-d_8 (0.350 mL) and PMe_3 (0.05 mL). The volatiles were removed to afford a white solid with spectroscopic features consistent with (^{Me4}PCP)Ir(CO)(PMe_3) (**6^{Me}**). ^{1}H NMR (300 MHz, C_6D_6): δ 7.09 (d; $^3J_{HP}$ = 7.3 Hz; 2H; Ar-*H*), 6.98 (d; $^3J_{HP}$ = 7.3 Hz ;1H; Ar-*H*), 3.25-2.73 (br m; 4H; Ar(-CH_2-)), 1.60-1.37 (br m; 12H; -P(CH_3)$_2$), 1.08 (d; 9H; -P(CH_3)$_3$). ^{31}P{^{1}H} NMR (121 MHz, C_6D_6): δ -0.92 (d; $^2J_{PP}$ = 112.4 Hz; 2P; -P(CH_2)(CH_3)$_2$), -55.9 (d; $^2J_{PP}$ = 112.4 Hz; 1P; -P(CH_3)$_3$). ^{13}C{^{1}H} NMR (176 MHz, C_6D_6): δ 192.3 (m; Ir-*C*O), 146.8 (m; C_{Ar}), 128.5 (s; C_{Ar}), 121.7 (s; C_{Ar}), 121.4 (m; C_{Ar}), 52.7 (m; -(CH_2)-), 25.7 (m; P(CH_3)$_2$), 24.4 (d; $^1J_{PC}$ = 20.0 Hz P(CH_3)$_3$), 21.5 (m; P(CH_3)$_2$). IR (solution, C_6D_6, cm^{-1}) ν(*CO*) 1923.

Conflicts of interest

There are no conflicts to declare

Acknowledgements

We thank Dr. Jonathan M. Goldberg, and Dr. Sophia D. T. Cherry for insightful discussions; Dr. Werner Kaminsky and Maike Blakely for the solution of the solid-state structure of **2^{Me}**, **trans-3^{Me}**, and **trans-7^{Me}**. This work was supported by the NSF under the Center for Enabling New Technologies through Catalysis CCI (CENTC) (CHE-1205189).

Notes and references

(1) Adams, J. J.; Arulsamy, N.; Roddick, D. M. *Organometallics* **2011**, *30*, 697-708.

(2) Ghosh, R.; Zhang, X. W.; Achord, P.; Emge, T. J.; Krogh-Jespersen, K.; Goldman, A. S. *J. Am. Chem. Soc.* **2007**, *129*, 853-866.

(3) Choi, J.; MacArthur, A. H. R.; Brookhart, M.; Goldman, A. S. *Chem. Rev.* **2011**, *111*, 1761-1779.

(4) Goldberg, J. M.; Cherry, S. D. T.; Guard, L. M.; Kaminsky, W.; Goldberg, K. I.; Heinekey, D. M. *Organometallics* **2016**, *35*, 3546-3556.

(5) Adams, J. J.; Arulsamy, N.; Roddick, D. M. *Dalton Trans.* **2011**, *40*, 10014-10019.
(6) Adams, J. J.; Lau, A.; Arulsamy, N.; Roddick, D. M. *Organometallics* **2011**, *30*, 689-696.
(7) Roddick, D. M. In *Organometallic Pincer Chemistry* 2012, 49-88.
(8) Adams, J. J.; Arulsamy, N.; Roddick, D. M. *Organometallics* **2012**, *31*, 1439-1447.
(9) Rybtchinski, B.; Ben-David, Y.; Milstein, D. *Organometallics* **1997**, *16*, 3786-3793.
(10) Lekich, T. T.; Askelson, P. G.; Burdick, R. K.; Heinekey, D. M. *Organometallics* **2018**, *37*, 211-213.
(11) Moulton, C. J.; Shaw, B. L. *J. Chem. Soc., Dalton Trans.* **1976**, 1020-1024.
(12) Jessop, P. G.; Morris, R. H. *Coord. Chem. Rev.* **1992**, *121*, 155-284.
(13) Li, S. H.; Hall, M. B. *Organometallics* **1999**, *18*, 5682-5687.
(14) Goldberg, J. M.; Wong, G. W.; Brastow, K. E.; Kaminsky, W.; Goldberg, K. I.; Heinekey, D. M. *Organometallics* **2015**, *34*, 753-762.
(15) Creaser, C. S.; Kaska, W. C. *Inorg. Chim. Acta* **1978**, *30*, L325-L326.
(16) Kundu, S.; Choliy, Y.; Zhuo, G.; Ahuja, R.; Emge, T. J.; Warmuth, R.; Brookhart, M.; Krogh-Jespersen, K.; Goldman, A. S. *Organometallics* **2009**, *28*, 5432-5444.
(17) Falivene, L.; Credendino, R.; Poater, A.; Petta, A.; Serra, L.; Oliva, R.; Scarano, V.; Cavallo, L. *Organometallics* **2016**, *35*, 2286-2293.
(18) Brewster, T. P.; Ou, W. C.; Tran, J. C.; Goldberg, K. I.; Hanson, S. K.; Cundari, T. R.; Heinekey, D. M. *ACS Catal.* **2014**, *4*, 3034-3038.
(19) Pahls, D. R.; Allen, K. E.; Goldberg, K. I.; Cundari, T. R. *Organometallics* **2014**, *33*, 6413-6419.
(20) Campos, J.; Kundu, S.; Pahls, D. R.; Brookhart, M.; Carmona, E.; Cundari, T. R. *J. Am. Chem. Soc.* **2013**, *135*, 1217-1220.
(21) Ou, W. C.; Cundari, T. R. *ACS Catal.* **2015**, *5*, 225-232.
(22) Lehman, M. C.; Pahls, D. R.; Meredith, J. M.; Sommer, R. D.; Heinekey, D. M.; Cundari, T. R.; Ison, E. A. *J. Am. Chem. Soc.* **2015**, *137*, 3574-3584.
(23) Fulmer, G. R.; Miller, A. J. M.; Sherden, N. H.; Gottlieb, H. E.; Nudelman, A.; Stoltz, B. M.; Bercaw, J. E.; Goldberg, K. I. *Organometallics* **2010**, *29*, 2176-2179.
(24) Roberto, D.; Cariati, E.; Psaro, R.; Ugo, R. *Organometallics* **1994**, *13*, 4227-4231.

Compared to analogous sterically demanding complexes, the methyl derived pincer iridium complex shows enhanced reactivity with H_2 including: rapid isomerization from a cis- to trans-dihydride complex and solvent activation during isomerization.